

## Rice husk derived silica and its application for treatment of fluoride containing wastewater: batch study and modeling using artificial neural network analysis

Swapnila Roy, Shubhalakshmi Sengupta, Suwendu Manna, Md. Azizur Rahman, Papita Das\*

Department of Chemical Engineering, Jadavpur University, 188, Raja S. C Mullick Road, Kolkata-700032, India,  
email: swapnilaroy@gmail.com (S. Roy), sengupta.shubha@gmail.com (S. Sengupta), suva84@gmail.com (S. Manna),  
mdazizur.rs@jadavpuruniversity.in (Md. A. Rahman), papitasaha@gmail.com (P. Das)

Received 30 October 2017; Accepted 8 February 2018

### ABSTRACT

Fluoride contamination in water may create environmental hazards. In the present investigation, nano silica was synthesized from agricultural waste (rice husk) at high temperature in a tubular reactor and de-fluoridation capacity of the entire product was explored. The batch experiments were conducted at different conditions: adsorbent dose, temperature, and contact time to evaluate the fluoride removal performance. It was observed that the synthesized product have higher de-fluoridation efficiency than its pristine counterparts such as 70.86% (rice husk, RH), 88.69% (rice husk derived silica, Si-RH) respectively. The equilibrium data for de-fluoridation by rice husk(RH) and rice husk derived silica (Si-RH) were best fitted to the Langmuir isotherm model. The experimental results were applied to obtain training set for Artificial Neural Network (ANN) analysis. The results suggested that ANN model prediction shows a closer interaction between experimental and theoretical results. It may be concluded that rice husk and its derivatives could be an environmentally benign and economic option for de-fluoridation.

*Keywords:* Fluoride; Silica derived from rice husk; Isotherm; Thermodynamic and kinetics study; Artificial neural network

### 1. Introduction

Fluorine is one of the essential trace elements for human health and its gaseous form is a strong oxidizing agent. The sources of industrial fluoride [1] are hydrofluoric acid, and ammonium bi-fluoride. Due to its electro negativity properties, it has very high affinity towards calcium (Ca). Depending on the fluoride concentration in the drinking water, duration of consumption has high impact on level of fluorosis both in children and adults especially old. Fluoride toxicity results when its consumption exceeds the threshold limit of 1.5 mg/L. Excessive consumption of fluoride results in dental and skeletal fluorosis [2–5]. Thus, de-fluoridation of water is required by using novel techniques. Decontamination of fluoride from water bodies was previously performed by adding lime followed by precipitation of fluoride in conventional method [6–8]. Different defluo-

ridation methods such as ion-exchange, electro coagulation, membrane filtration and adsorption [9–14] used for the de-fluoridation of water. Usage of different types of adsorbents such as charcoal, tamarind seed, agricultural waste materials, bermuda grass, ionic resin etc. are also used for fluoride removal. However, there is a difference between efficiency of removal between carbonized and chemically treated forms of these adsorbents [15,16].

In India, rice is produced in large quantities and the husk of it is considered as agricultural waste material. Due to large production of rice, rice husk became a by-product. The composition of the rice husk is mainly cellulose, hemicelluloses, lignin, silica and crude protein. Silica is one of the important ingredient of the rice husk, chemically present as silicon-cellulose membrane which mainly acts to protect from microbial attack. Silica has some commercial value, and if this silica can be extracted from rice husk, then waste husk [17] can be utilized further and as a result the discharge problem of rice husk can be minimized. In this

\*Corresponding author.

study, silica was extracted from rice husk and was used further to treat fluoride containing solution. Rice husk was also used as adsorbent in this study and a comparison between the rice husk and silica's efficiency to remove the fluoride present in solution was studied.

The physical and chemical properties of the prepared silica extracted from rice husk were determined and de-fluoridation efficiency was estimated using different experimental procedure by adsorption as a function of contact time, adsorbent dose and temperature. The main advantage of the current process is high removal efficacy of the modified materials. The modification processes used in this study improve the pore volume and surface structure of the materials which may improve their fluoride removal efficacy. The process is novel because the raw materials is cheap, easily available, the removal efficacy of the materials can be improved significantly with minimal intervention and most importantly the process does not produce any toxic sludge. To evaluate the mechanism of the removal using both the adsorbent, thermodynamics and kinetics studies [18,19] were also used for optimization of the de-fluoridation efficiency. ANN analysis [20–23] was applied to achieve the removal of fluoride [24] using the three adsorbents. For this artificial neural network with three process parameters (temperature, time and amount of adsorbent used), one output response was considered. In this case, back-propagation method was used, based on Levenberg–Marquardt algorithm.

## 2. Materials and methods

### 2.1. Sample collection

The raw materials (rice husk) had been bought from local rice mill, Kolkata. The physico chemical properties of rice husk [25] were estimated by proximate and ultimate analyses. Proximate analysis has been performed following American Society for Testing Materials (ASTM, 1994).

### 2.2. Materials

Sodium Hydroxide [Merck, Germany], Hydrochloric acid (HCl), sodium fluoride [Merck, Germany]. All chemicals of reagent grade and ultra pure distilled water were used in all the preparations.

### 2.3. Preparation of adsorbents

#### 2.3.1. Silica extraction

Firstly, rice husk was washed with sodium dodecyl sulfate (SDS) solution for 10 min to remove different impurities. Then, the rice husk was purified by double distilled water to remove that surfactant. It was initially dried at room temperature and then at 383 K for 1 d. This treated rice husk is designated as un-leached rice husk. The obtained dried rice husk was taken in the crucible for thermal treatment in the range of 873–973 K to increase the relative amount of silicon oxide by reduction of carbonaceous materials. Then the rice husk was converted to ash (RHA) form. Then this RHA was taken in 250 ml covered

Erlenmeyer flask where it was purified by double distilled water followed by addition of 1 N NaOH solution. This solution was stirred for 1 h in boiling condition, followed by filtration. The filtrates and washings were cooled down to room temperature. Then the solution was stirred by 1 N HCl to make pH 6–7. The Silica started to precipitate gradually and it was agitated for 18 h. After that excess HCl was added by stirring to make pH 2–3. Finally, it was filtered, oven dried and stored in the container for further study [26,27]. This obtained silica gel is designated as acid leached silica.

### 2.4. Characterization techniques

The Scanning Electron Microscopy of the sample was conducted using JEOL-JSM-6360 (Jeol, Japan). SEM analysis was carried out to study the changes in surface morphology such as smoothness and roughness of acid-leached Si-RH [28]. The sample was coated with platinum evaporative coating under high vacuum at 15 kV with 15 mm working distance. The infrared spectra of the adsorbent were recorded using Fourier Transform Infrared Spectrometer (Perkin Elmer Spectrum, United Kingdom) in transmittance mode. The KBr pressed pellet technique was used to record the spectrum IR range of 500–4000  $\text{cm}^{-1}$ . X-ray diffraction (XRD) analysis of the sample was performed out using an X-ray diffractometer (Bruker, D8 Advance, Germany) with Cu  $K\alpha$  radiation at an accelerating voltage 40 kV and emission current 30 mA in the range of diffraction angle  $2\theta = 5 - 80^\circ$ . For TEM analysis, sample analysis was conducted as usual method and the image achieved with a transmission electron microscope (JEOL, Japan; Model No. JEM 2100 HR with EELS) revealed the size and structure of the extracted silica [29].

## 3. Experimental

### 3.1. Experimental set up

In this study, batch experiments were conducted by using initial fluoride concentration 50  $\text{mg L}^{-1}$  of volume 100 mL within a 250 mL PTFE (Polytetra fluoroethylene) conical flasks. Here these three adsorbents were mixed in the 100 mL fluoride solution in different concentration such as (0.2  $\text{g L}^{-1}$ , 0.75  $\text{g L}^{-1}$ , 0.5  $\text{g L}^{-1}$ , 1  $\text{g L}^{-1}$ , 1.5  $\text{g L}^{-1}$ ) within 303–343 K (range of temperature), 20–180 min (range of contact time), to obtain optimized condition for adsorbent dose ( $\text{g/L}$ ), contact time (min) and temperature (K), respectively.

Batch experiments were performed in temperature controlled incubator shaker (INNOVA 4430, New Brunswick Scientific, Canada). Temperature fluctuations in the reactor were negligible. Representative samples were collected from the flasks in particular time interval for decontamination of fluoride in solution by using ion-meter (Thermo Scientific Orion ion-meter, USA).

Following equation was used to calculate percentage fluoride removal efficiency of adsorbents:

$$R(\%) = \frac{C_i - C_0}{C_i} \times 100 \quad (1)$$

Here  $C_i$  denotes initial fluoride concentration ( $\text{mg L}^{-1}$ ) and  $C_0$  denotes final fluoride concentration in solution ( $\text{mg L}^{-1}$ ).

### 3.2. Batch sorption experiment

In this present batch study, the required quantity of RH, Si-RH were added to the fluoride solution, then it was stirred for different contact time with different dosage of adsorbent at different temperature. All experiments were carried out in thrice and the relative standard deviation (RSD) is within 10 numerically.

### 3.3. Determination of point of zero charge ( $\text{pH}_{\text{PZC}}$ )

The pH at the potential of zero point charge ( $\text{pH}_{\text{zpc}}$ ) [30] of the sample was measured using the pH drift method using batch equilibrium method. Nitrogen was bubbled through the solution at  $25^\circ\text{C}$  to remove dissolved carbon dioxide until the initial pH stabilizes. In this case 0.1 M NaCl was selected as electrolyte. The initial pH ( $\text{pH}_{\text{initial}}$ ) (2–12) of NaCl solution was adjusted using required amount of 0.1 M HCl or NaOH. 0.1 g of silica was added to 20 ml of 0.1 M NaCl solution and then it was agitated continuously for 1 day at room temperature. After 24 h the solution was filtered and final pH ( $\text{pH}_{\text{final}}$ ) were recorded. The graph of final pH versus initial pH was used to determine the point at which the initial pH and final pH values were equal. The point of zero charge ( $\text{pH}_{\text{PZC}}$ ) of adsorbent was estimated from the point of intersection of the curve ( $\text{pH}_{\text{final}}$  Vs  $\text{pH}_{\text{initial}}$ ).

### 3.4. Thermodynamic, kinetics and isotherm studies

#### 3.4.1. Adsorption isotherms

The Freundlich isotherm constants were estimated using the following equation:

$$\log q_e = \log K_F + \left(\frac{1}{n}\right) \log C_e \quad (2)$$

Here  $q_e$  indicates the amount of fluoride adsorbed at equilibrium, and  $K_F$  and  $n$  are Freundlich constants indicating adsorption capacity and adsorption intensity, respectively.

In case of Langmuir isotherm, the following equation was applied:

$$\frac{C_e}{q_e} = \frac{C_e}{q_m} + \frac{1}{K_L q_m} \quad (3)$$

Here  $q_e$  indicates the amount of fluoride adsorbed at equilibrium ( $\text{mg L}^{-1}$ ),  $C_e$  is the concentration of fluoride in the aqueous phase at equilibrium ( $\text{mg L}^{-1}$ ).  $K_L$  and  $q_m$  denote the Langmuir constants related to energy of adsorption and the adsorption capacity respectively.

#### 3.4.2. Adsorption kinetics

Adsorption kinetics was estimated using pseudo 1<sup>st</sup> order and 2<sup>nd</sup> order kinetics equations.

The pseudo 1<sup>st</sup> order rate constant was calculated using the following equation:

$$\frac{dq_t}{dt} = k_1 (q_e - q_t) \quad (4)$$

where  $q_e$  indicates fluoride adsorbed at equilibrium per unit weight of adsorbent ( $\text{mg g}^{-1}$ ),  $q_t$  denotes the amount of fluoride adsorbed at any instant ( $\text{mg g}^{-1}$ ) and  $k_1$  is the rate constant ( $\text{min}^{-1}$ ).

Integrating at these conditions as  $t = 0$  and  $q_t = 0$  to  $t = t$  and  $q_t = q_t$ , the final equation can be expressed as:

$$\log(q_e - q_t) = \log q_e - \frac{k_1}{2.303} t \quad (5)$$

The pseudo 2<sup>nd</sup> order rate constant was derived from the following equation:

$$\frac{t}{q_t} = \frac{1}{k_2 q_e^2} + \frac{1}{q_e} t \quad (6)$$

where  $k_2$  denotes the pseudo 2<sup>nd</sup> order rate constant of adsorption ( $\text{g mg}^{-1} \text{min}^{-1}$ ) and  $q_e$  and  $q_t$  are the amounts of fluoride adsorbed ( $\text{mg g}^{-1}$ ) at equilibrium and at time  $t$  respectively.

### 3.5. Adsorption thermodynamics

Thermodynamic parameters such as changes in Gibbs free energy ( $\Delta G^\circ$ ;  $\text{kJ mol}^{-1}$ ), enthalpy ( $\Delta H^\circ$ ;  $\text{kJ mol}^{-1}$ ) and entropy ( $\Delta S^\circ$ ;  $\text{J mol}^{-1} \text{K}^{-1}$ ) were calculated as follows:

$$K_c = \frac{C_a}{C_e} \quad (7)$$

$$\Delta G^\circ = -RT \ln K_c \quad (8)$$

$$\Delta G^\circ = \Delta H^\circ - T \Delta S^\circ \quad (9)$$

where  $K_c$  is the coefficient of distribution for the adsorption;  $C_a$  is fluoride adsorbed per unit mass of the adsorbent ( $\text{mg L}^{-1}$ ) and  $C_e$  is equilibrium concentration of adsorbate in aqueous phase ( $\text{mg L}^{-1}$ ),  $R$  is universal gas constant ( $8.314 \text{ J mol}^{-1} \text{K}^{-1}$ ) and  $T$  is absolute temperature (K).

## 4. Results and discussion

### 4.1. Physico chemical properties of adsorbents

The results of the physico chemical analysis of the Si-RH are represented in Table 1. The surface of silica had negative charged in aqueous solution as its pH was above the pH in the point of zero charge ( $\text{pH}_{\text{PZC}}$ ). It indicates that adsorbent has cationic exchange capacity. The bulk density of silica was lower than  $1.5 \text{ g cm}^{-3}$ , which indicated that it was lightweight material.

#### 4.1.1. Proximate and ultimate analysis results of rice husk

The results are represented in Table 2. The ash and fixed carbon of rice husk was stimulated for the production of

Table 1  
Results of physicochemical analysis of Si-RH

Serial No.	Characteristics	Si-RH
1	Moisture content (%)	6.32
2	pH	5.7
3	Bulk Density	0.32
4	Porosity	0.79
5	pH(PZC)	5.2

Table 2  
Proximate and ultimate analysis results of collected rice husk

Ultimate (wt %, dry)	Proximate (wt%)
Carbon 33.23	Volatile matter 48.59
Nitrogen 0.38	Fixed carbon 15.36
Hydrogen 2.3	Ash 18.69
Oxygen 29.67	
Sulphur 0.0	

silica. The content of each of parameter varies on different criteria such as nature of rice husk, chemical properties of soil, weather etc. Here the fixed carbon (12–18) and ash content were within the range.

#### 4.2. Characterization of silica extracted from rice husk

It is clearly observed [31] from Fig. 1A that amorphous silica has porous structure which can be attributed to the burning out of carbonaceous matter within the rice husk during combustion. The smaller particles had affinity to form aggregation. The polymerization of hydrated silica to form skeletal silica network which can be explained by SEM image. From Fig. 1B it is observed that significance peak was observed at  $1200\text{ cm}^{-1}$  indicating Si-OR bond.

From Fig. 1C it is observed that a significant peak was observed around  $25^\circ$  indicating silicon di-oxide (JCPDS ref: 98–007–56). From TEM image (Fig 1D) it is observed that the particle is round in shape with porous structure and size of the extracted silica is  $429\text{ nm}$ – $500\text{ nm}$  in range. The size of the particle was also analysed using Zeta sizer (Malvern. UK) and Z average size was  $424\text{ nm}$ . In the case of Si-RH, with increas-

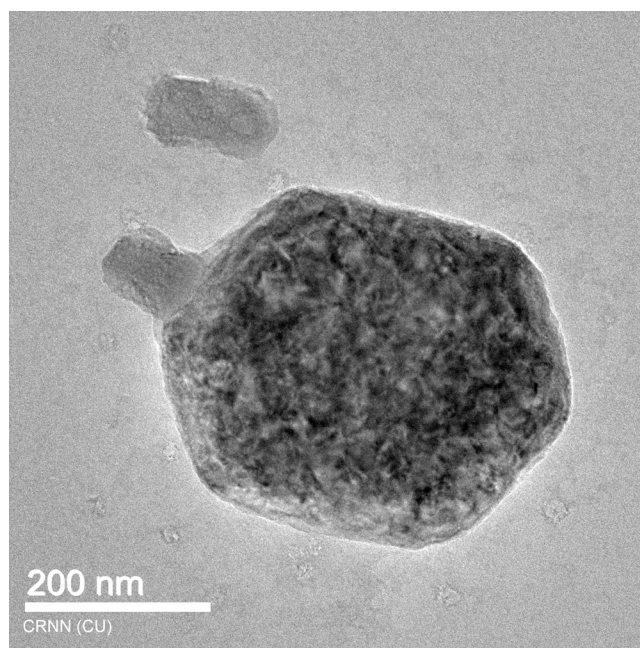
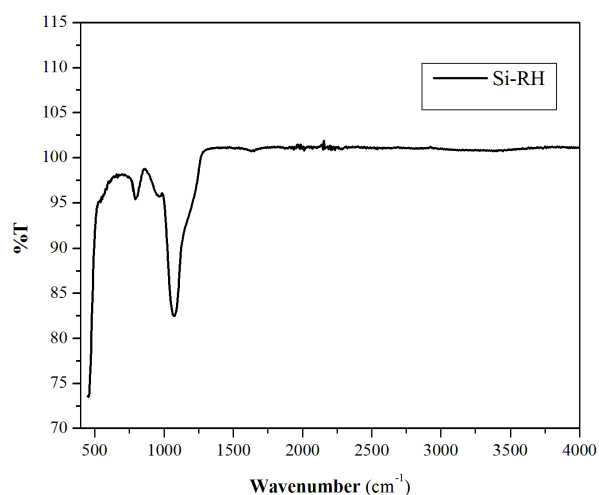
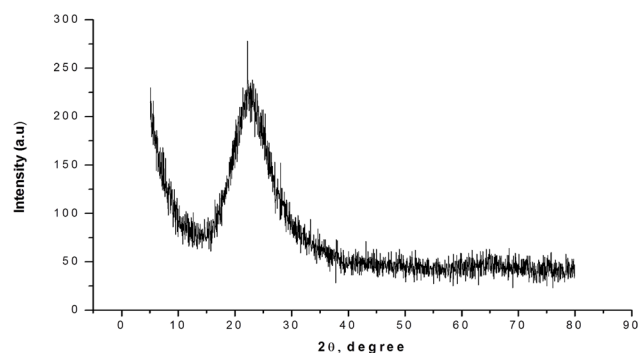
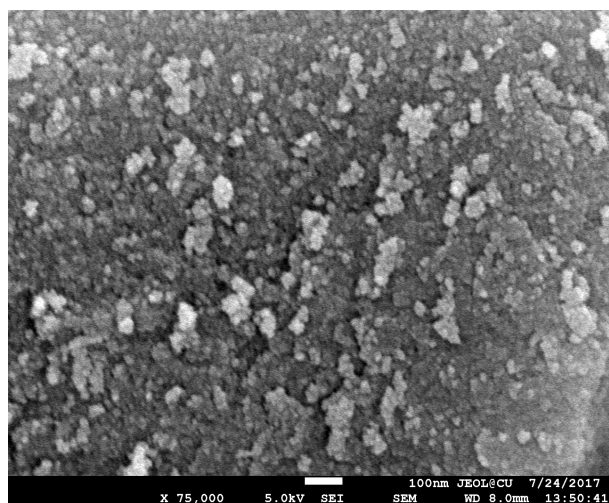


Fig. 1. Include (A) SEM of Silica from Rice husk, (B) XRD of extracted silica, (C) FTIR of rice husk extracted silica, (D) TEM image of silica.

ing concentration of NaOH and temperature for pyrolysis amount of extracted silica content increased. Chemically it can be explained by the fact that (Si–O–C/Si–O–Si) bonds, fragmented with increasing temperature. Consequently, silica yield increased due to broken Si–O bonds.

#### 4.3. Batch adsorption study

##### 4.3.1 Effect of contact time

Comparing three plots (Fig. 2) it is observed that on increasing the time from 20 to 60 min, removal increased. As the time increased, more fluoride ions can be attached on the surface because of attraction force which resulted in fluoride removal. But after certain time (60 min), removal decreased due to saturation of adsorbent surface, so beyond that point the repulsive force may be activated in between fluoride ion and adsorbent surface.

##### 4.3.2. Effect of adsorbent dose

It is observed in Fig. 3 that Si-RH is the best adsorbent for de-fluoridation than RH. De-fluoridation efficiency

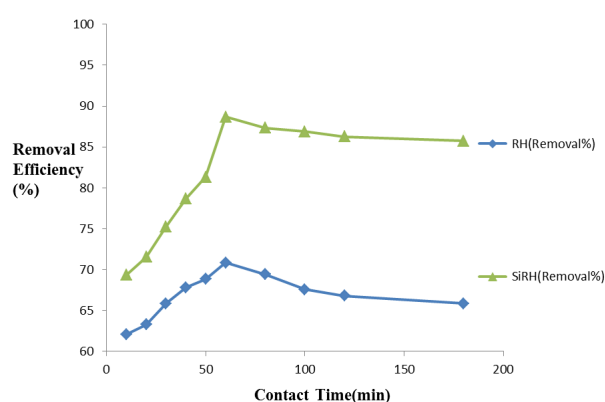


Fig. 2. Effect of contact time on de-fluoridation by RH, Si-RH (experimental conditions,  $C_0 = 50 \text{ mg}\cdot\text{L}^{-1}$ , agitation speed = 150 rpm  $T = 333 \text{ K}$ , adsorbent dose = 10 g/L).

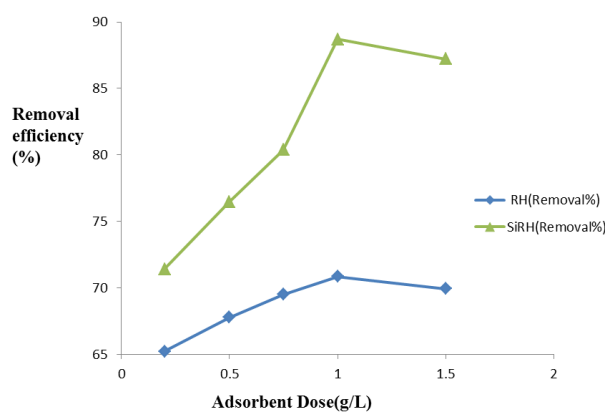


Fig. 3. Effect of adsorbent dose on de-fluoridation by RH, Si-RH (experimental conditions,  $C_0 = 50 \text{ mg}\cdot\text{L}^{-1}$ , agitation speed = 150 rpm  $T = 333 \text{ K}$ , contact time: 60 min).

increased within 0.2 g–1.5 g  $\text{L}^{-1}$  firstly increased, and then decreased. The de-fluoridation efficiency firstly increased because of the increase number of active surface sites responsible of fluoride attachment. But as adsorbent dose was increased, the relative lower concentration of fluoride with respect to the surface active sites made the ions unavailable.

##### 4.3.3. Effect of temperature

It was experimentally proved (Fig. 4) that with increasing temperature, the percent removal of fluoride gradually increased from 303K to 343K. After 333K, de-fluoridation efficiency decreased. For temperature increased between 303K and 343K possible broadening of pores enhanced the fluoride diffusion which increased the removal efficiency. But as temperature increased beyond 333K, the enhanced Brownian motion of the fluoride ions and further broadening of pores increase the diffusion of attached fluoride.

##### 4.3.4. Effect of pH

The solution pH is significant monitoring parameter, driving an adsorption process. In present study, the effect of pH on removal efficiency of fluoride was experimented. According to pH of solution containing adsorbent and adsorbate, protonation/deprotonation was occurred. The effect of pH on fluoride adsorption is likely due to the charged properties of both adsorbate and adsorbent. From the batch equilibrium study, it was observed that rate of removal efficiency was decreased with an increase in pH of fluoride solution and maximum efficiency was found at around pH 2.0 (88.69%). Further decrease in pH (<2), did not remarkably change fluoride removal capacity (Fig. 5A). It can be illustrated that both adsorbents retained its high adsorption efficiency at acidic pH. This may be attributed due to electrostatic interaction between cationic surface with negatively charged fluoride. As pH increased, the adsorption capacity may be reduced due to deprotonation of fluoride in alkaline medium in presence of excess  $\text{OH}^-$  ions which may compete with negatively charged fluoride

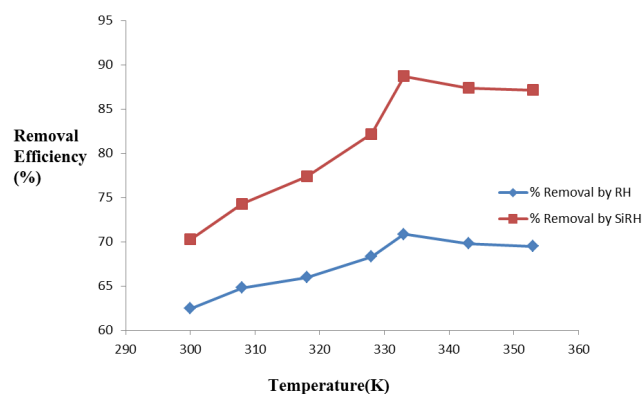


Fig. 4. Effect of temperature on de-fluoridation by RH, Si-RH (experimental conditions,  $C_0 = 50 \text{ mg}\cdot\text{L}^{-1}$ , agitation speed = 150 rpm adsorbent dose = 10 g/L, contact time: 60 min).

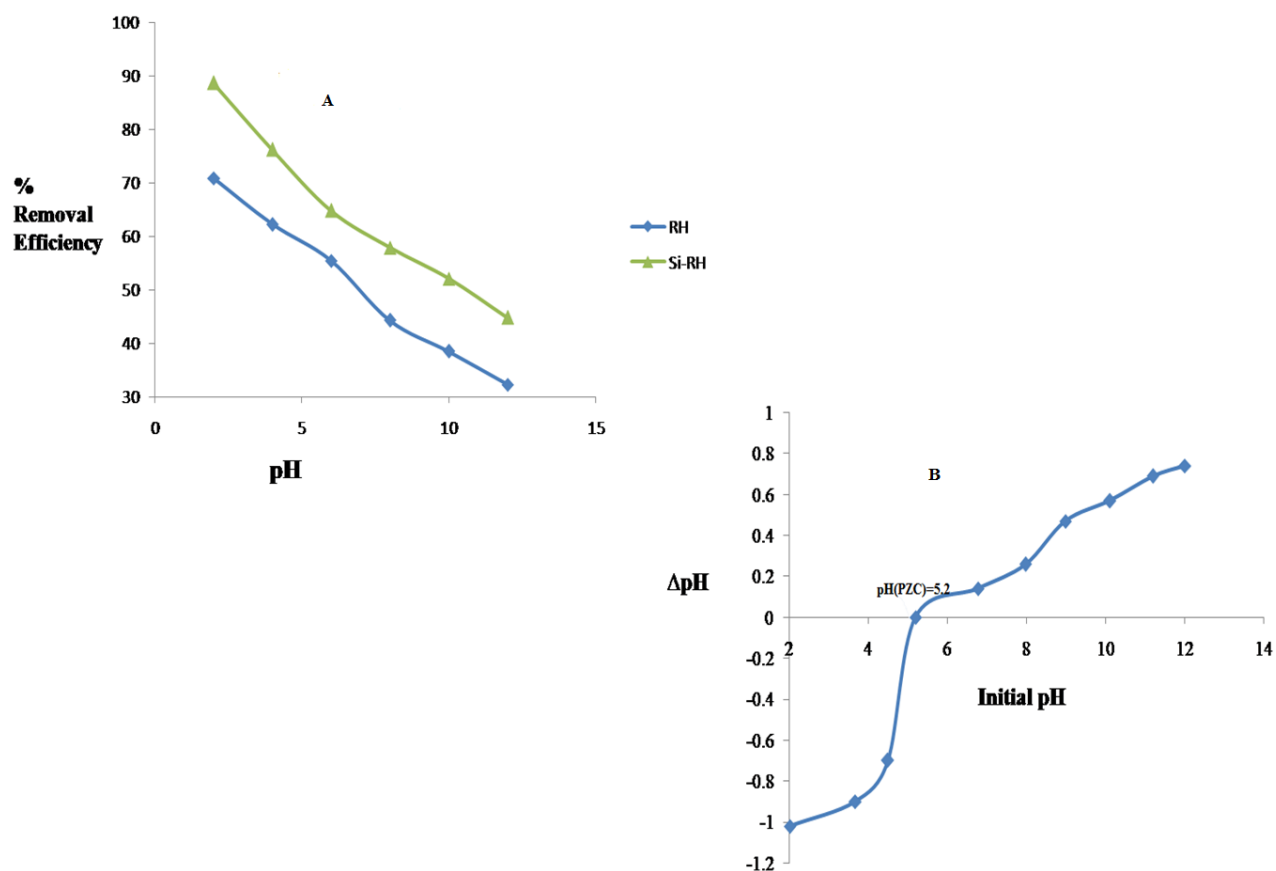


Fig. 5. (a) Effect of pH on de-fluoridation by RH (experimental conditions:  $C_0 = 50 \text{ mg L}^{-1}$ , agitation speed = 150 rpm, adsorbent dose = 1.0 g/L, contact time: 60 min,  $T = 333 \text{ K}$ ) (b) Determination of pH (PZC) by Si-RH.

ion. Fig. 5B shows that  $\text{pH}_{\text{PZC}}$  of silica was 5.2. Since it was found to be 5.2, so at any  $\text{pH} < \text{pH}_{\text{PZC}}$ , the surface of rice husk derived silica is positively charged and  $\text{pH} > \text{pH}_{\text{PZC}}$ , the surface of silica is negatively charged.

#### 4.4. Estimation of different thermodynamic and kinetic parameter

##### 4.4.1. Effect of adsorption isotherms

In the case of RH and Si-RH, Langmuir adsorption isotherms resulted in a straight line between  $C_e$  vs.  $C_e/Q_e$  (Figs. 6A,B) with  $R^2$  values of 0.9989 and 0.9952 respectively, hence indicating the suitability of RH and Si-RH for the adsorption of fluoride. The equilibrium data [32] for rice husk derived silica had been analyzed by linear regression of Langmuir isotherm model equations (Fig. 6C). In case of RH and Si-RH, Freundlich isotherm (Fig. 7A,B), straight line ( $\log Q_e$  vs.  $\log C_e$ ) were also obtained for all adsorbents having  $R^2$  values of 0.9631 and 0.9191 respectively. The related parameters obtained by calculation from the values of slopes and intercepts of the respective linear plots are shown in Table 3.

The present data indicated that the adsorption of fluoride is due to the Langmuir monolayer surface adsorption. Because the Freundlich isotherm model, based on multilayer adsorption, explained the data well fitted within  $R^2$

values in between 0.994–0.997. But here it was not within that range. Comparing  $R^2$  values between these isotherms it can be said that the adsorption of fluoride [33] had better compatibility with Langmuir adsorption model which indicated formation of mono layer on the adsorbents surface. Mathematically based on Eqs. (2) and (3) the values of  $K_F$ ,  $n$ ,  $Q_e$  and  $b$  are reported in Table 3.

The adsorption system is favourable or unfavourable depends on the effect of isotherm shape

The essential features of the Langmuir isotherm can be expressed in terms of a dimensionless constant separation factor or equilibrium parameter  $R_L$  which is defined by the following relationship:

$$R_L = \frac{1}{(b + C_0)} \quad (10)$$

where  $R_L$  is a dimensionless separation factor,  $C_0$  is the initial fluoride concentration (mg/L) and  $b$  is the Langmuir constant (L/mg). The parameter  $R_L$  indicated the type of isotherm accordingly.

$R_L > 1 \rightarrow$  Unfavorable

$R_L = 1 \rightarrow$  Linear

$0 < R_L < 1 \rightarrow$  Favorable

$R_L = 0 \rightarrow$  Irreversible

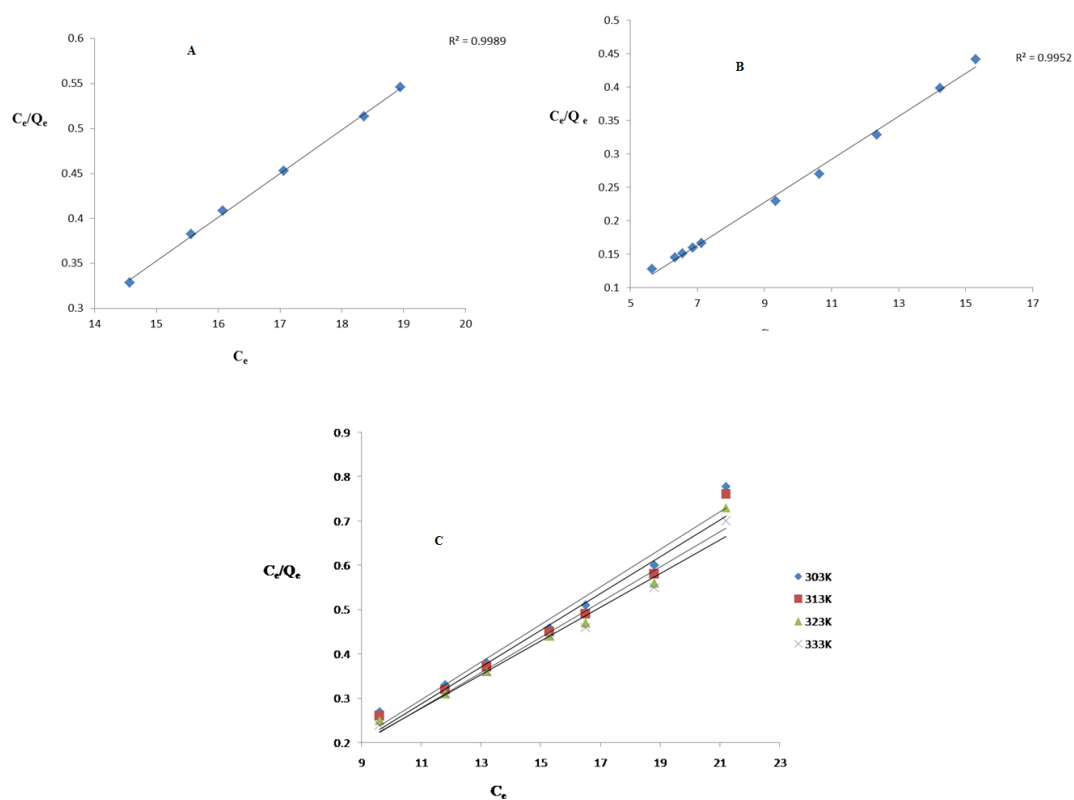


Fig. 6. Langmuir adsorption isotherm plots of de-fluoridation onto (A) RH (B) Si-RH (C) langmuir isotherms obtained by using linear r method for the adsorption of fluoride using Si-RH at various temperatures.

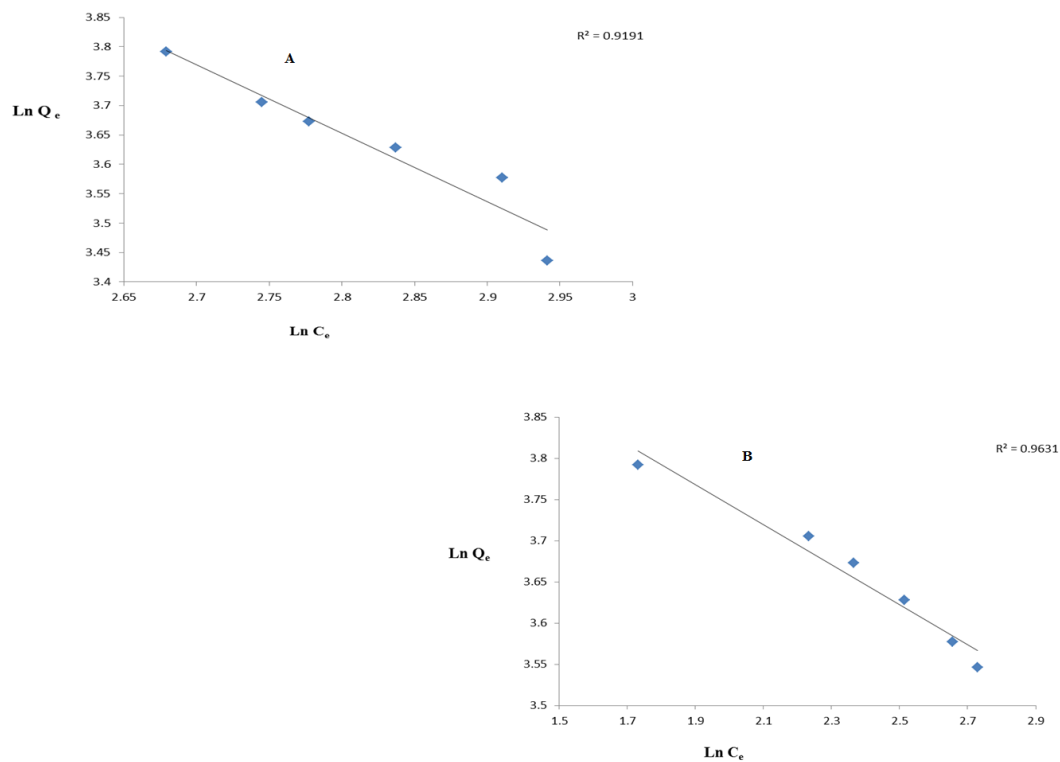


Fig. 7. Freundlich adsorption isotherm plots of de-fluoridation onto (A) RH (B) Si-RH.

Table 3  
Investigating different isotherm parameters for fluoride adsorption by silica and rice husk

Models	Parameters	Description	Silica	Rice husk
Langmuir	$C_e$	Equilibrium fluoride concentration in solution, mg L <sup>-1</sup>	5.66	14.57
	$q_e$	Theoretical maximum adsorption capacity, mg g <sup>-1</sup>	44.35	21.5
	$Q_0$	Maximum monolayer coverage capacity calculated from slope of $C_e/q_e$ vs. $C_e$ plot, mg g <sup>-1</sup>	4.212	2.076
	$b$	Langmuir coefficient of energy of adsorption calculated from intercept of $C_e/q_e$ vs. $C_e$ plot, L mg <sup>-1</sup>	0.064	0.39
	$R^2$	Correlation coefficient	0.9952	0.9989
Freundlich	$n_f$	Adsorption intensity calculated from slope of $\ln q_e$ vs. $\ln C_e$ plot	0.28	1.2
	$K_f$	Freundlich coefficient of adsorption capacity calculated from intercept of $\ln q_e$ vs. $\ln C_e$ plot, mg g <sup>-1</sup>	4.31	6.07
	$R^2$	Correlation coefficient	0.9191	0.9631

Table 4  
 $R_L$  values at different temperatures calculated using Langmuir constants

Initial concentration of fluoride ( $C_0$ ) mg/L	303 K	313K	323K	333K
5	0.54	0.5	0.46	0.41
7.5	0.45	0.4	0.36	0.31
10	0.33	0.29	0.26	0.23
12	0.21	0.19	0.18	0.15
15	0.11	0.09	0.08	0.06

The relationship between  $R_L$  and  $C_0$  was presented in Table 4 to show the essential features of the Langmuir isotherm [33]. In this investigation, the  $R_L$  values calculated in the range of fluoride concentration are estimated to be in the range of 0.06–0.54, which suggested the favourable adsorption of fluoride onto Si-RH, under the conditions used for the experiments.

#### 4.4.2. Effect of adsorption kinetics at different temperature

In this investigation, the pseudo-first order kinetic equation did not fit well in the whole range of interaction time by plotting of  $\ln(q_e - q_t)$  vs.  $t$  (Figure not shown). As the applicability of the first order kinetics become untenable, then the adsorption may follow second order kinetics.

Pseudo-second-order kinetic model is based upon the assumption that it is a one-step process, and the rate-limiting step may be chemical adsorption, involving valence forces by sharing or exchanging electrons between the adsorbent and adsorbate. The pseudo-second order equation is based on the adsorption capacity on the solid phase.

The linear plots of  $t/q_t$  vs.  $t$  are shown in Fig. 8. It was observed that as temperature increased from 303 to 333 K, removal of fluoride efficiency increased. The rate constant  $k_2$  (g/mg·min) and  $q_e$  (mg/g) for the adsorption of F<sup>-</sup> ions were evaluated from the intercept and slope of the linear kinetic plots between  $t/q_t$  and time (Fig. 8). A high correla-

tion coefficient ( $R^2$ ) and rate constant  $k_2$  g/(mg·min) were obtained from the pseudo-second-order kinetics equation, indicating that due to increase in the mobility of fluoride due to temperature rise, the adsorption capacity increased. It was observed that with increased in time, the fluoride adsorption also increased for both adsorbents up to 333K. The plot of  $t/q_t$  vs  $t$  showing linear plot with regression coefficient of 0.999 and 0.9987 for RH and Si-RH, respectively (Tables 5A, 5B).

So pseudo second order kinetic model deserved main attention in this investigation because the nature of adsorption over the whole range of this investigation supported pseudo-second order kinetic equation.

#### 4.5. Thermodynamic parameters

From the experimental results it is observed from Table 6 that  $\Delta G^\circ$  increased with increasing temperature indicating adsorption was thermodynamically feasible in nature. Positive values of  $\Delta H^\circ$  implied the endothermic nature of the reaction. Negative value of  $\Delta G^\circ$  in all cases representing adsorption reaction was spontaneous in nature. In this case,  $\Delta G^\circ$  decreased up to 333 K and after that it increased indicating adsorption reaction was feasible up to 333 K. As the reaction was endothermic in nature, uptake capacity of fluoride ions was increasing with temperature. But after 333 K, the reverse reaction occurred. Entropy of the reaction was estimated from the experimentally obtained data and was positive. Enthalpy for each case was positive indicating that the process was spontaneous in nature. Corresponding entropy was 179.6, 191.1 J mol<sup>-1</sup> K<sup>-1</sup> for RH and Si-RH respectively.

#### 4.6. Artificial neural network analysis

Matlab 7 was used in this case to obtain the most appropriate network model to remove fluoride containing wastewater using the rice husk and extracted silica from it. Trial and error method was used in this case. In this study, feed-forward neural network with three inputs (temperature, time and amount of adsorbent used), two hidden layers and one output layer (including

Table 5A  
Analysis of kinetic parameters for fluoride adsorption by rice husk

Models	Parameters	Description	Temperatures (°C)			
			35	45	55	60
Pseudo first order	$k_1$	Pseudo-1 <sup>st</sup> order rate constant obtained from linear plots of $\log(q_e - q_t)$ vs. $t$ , min <sup>-1</sup>	0.0015	0.0018	0.0022	0.0023
	$q_e$ (cal)	Quantity of fluoride adsorbed at equilibrium, mg g <sup>-1</sup>	2.37	3.46	5.27	6.92
	$R^2$	Correlation coefficient	0.602	0.683	0.792	0.862
Pseudo second order	$k_2$	Pseudo-2 <sup>nd</sup> order rate constant determined from plot of $t/q_{res} \cdot t$ , mg g <sup>-1</sup> min <sup>-1</sup>	0.03	0.04	0.05	0.06
	$q_e$	Quantity of fluoride adsorbed at equilibrium, mg g <sup>-1</sup>	17.57	19.68	24.35	26.22
	$R^2$	Correlation coefficient	0.9412	0.9537	0.9831	0.999

Table 5B  
Analysis of kinetic parameters for fluoride adsorption by rice husk derived silica

Models	Parameters	Description	Temperatures (°C)			
			35	45	55	60
Pseudo first order	$k_1$	Pseudo-1 <sup>st</sup> order rate constant obtained from linear plots of $\log(q_e - q_t)$ vs. $t$ , min <sup>-1</sup>	0.0014	0.0016	0.0019	0.0022
	$q_e$ (cal)	Quantity of fluoride adsorbed at equilibrium, mg g <sup>-1</sup>	1.28	2.34	4.76	6.78
	$R^2$	Correlation coefficient	0.635	0.724	0.786	0.803
Pseudo second order	$k_2$	Pseudo-2 <sup>nd</sup> order rate constant determined from plot of $t/q_{res} \cdot t$ , mg g <sup>-1</sup> min <sup>-1</sup>	0.02	0.03	0.04	0.05
	$q_e$	Quantity of fluoride adsorbed at equilibrium, mg g <sup>-1</sup>	15.47	17.24	19.57	21.22
	$R^2$	Correlation coefficient	0.9511	0.9614	0.9821	0.9987

Table 6  
Thermodynamic parameters for the adsorption of fluoride onto RH and Si-RH

Serial No.	T, K	$\Delta G^\circ$ (kJ/mol)		$\Delta H^\circ$ (kJ/mol)		$\Delta S^\circ$ (J/(mol K))	
		RH	Si-RH	RH	Si-RH	RH	Si-RH
1	303	-8.93	-9.03	46.3	50.33	179.6	191.1
2	313	-10.23	-10.93				
3	328	-12.15	-12.54				
4	333	-13.02	-13.29				
5	343	-11.65	-11.56				

one neuron) was considered. In this case, the data was trained using back-propagation method based on Levenberg–Marquardt algorithm. Here, linear transfer function i.e POSLIN was chosen as input to hidden layer, and PURELIN was chosen for transfer function between hidden to output layer for mapping the data. Experimental and the ANN predicted response is shown in Figs. 9A,B. It is observed that in all the cases the correlation coefficient was higher than 0.88 indicating the reliability of the developed ANN model.

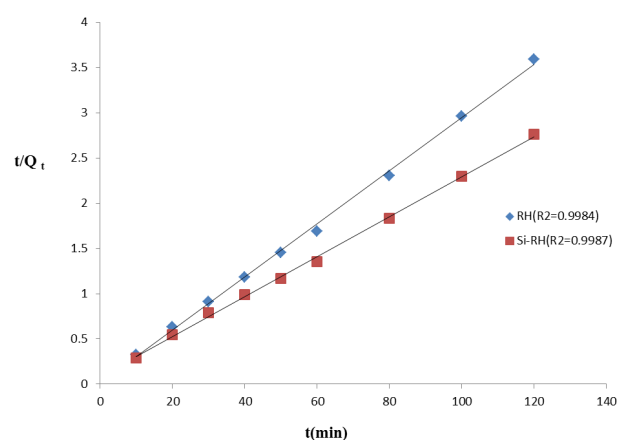


Fig. 8.

## 5. Conclusion

In this present study, rice husk and silica extracted from rice husk was used for treatment of fluoride containing wastewater. It was observed that extracted silica has efficiency for removal of fluoride present in solution. It was

also observed that the removal technique follows Langmuir adsorption isotherm indicating the process was mono layer surface adsorption. The process followed 2<sup>nd</sup> order kinetics and it was spontaneous in nature and all the adsorbent could be used as efficient adsorbent for the treatment of fluoride containing wastewater present in solution.

### Acknowledgment

This study was supported by Chemical Engineering Department, Jadavpur University, Kolkata, India and West Bengal Pollution Control Board, India. Authors are thankful for their support and service. Authors would like to acknowledge Prof. Aniruddha Mukhopadhyay, Department of Environmental Science, University of Calcutta, Kolkata for the characterization facilities. SS would like to acknowledge UGC D S kothari Postdoctoral scheme (Sanction no: CH/15-16/0163) for financial assistance.

### References

- [1] I. Ponsot, R. Falcone, E. Bernardo, Stabilization of fluorine-containing industrial waste by production of sintered glass-ceramics, *Ceram Int.*, 39 (2013) 6907–6915.
- [2] H. Chen, M. Yan, X. Yang, Z. Chen, G. Wang, D. Schmidt-Vogt, Y. Xu, J. Xu, Spatial distribution and temporal variation of high fluoride contents in groundwater and prevalence of fluorosis in humans in Yuanmou County, Southwest China, *J. Hazard Mater.*, 235–236 (2012) 201–209.
- [3] Z. Mandinic, M. Curcic, B. Antonijevic, C.P. Lekic, M. Carevic, Relationship between fluoride intake in Serbian children living in two areas with different natural levels of fluorides and occurrence of dental fluorosis, *Food Chem Toxic.*, 47 (2009) 1080–1084.
- [4] Z. Mandinic, M. Curcic, B. Antonijevic, M. Carevic, J. Mandic, D. Djukic-Cosic, C.P. Lekic, Fluoride in drinking water and dental fluorosis, *Sci. Total Environ.*, 408 (2010) 3507–3512.
- [5] B. Wang, B. Zheng, C. Zhai, G. Yu, X. Liu, Relationship between fluorine in drinking water and dental health of residents in some large cities in China, *Environ. Int.*, 30(2004) 1067–1073.
- [6] M. Sarkar, A. Banerjee, P.P. Pramanick, A.R. Sarkar, Use of laterite for the removal of fluoride from contaminated drinking water, *J. Colloid Interface Sci.*, 302 (2006) 432–441.
- [7] F. Shen, X. Chen, P. Gao, G. Chen, Electrochemical removal of fluoride ions from industrial wastewater, *Chem. Eng. Sci.*, 58 (2003) 987–993.
- [8] M.G. Sujana, R.S. Thakur, S. Das, N. Rao, S.B. De-fluorination of waste water, *Asian J. Chem.*, 4 (1997) 561–570.
- [9] S. Sobhanardakani, R. Zandipak, Adsorption of Ni(II) and Cd(II) from aqueous solutions using modified rice husk, *Iran. J. Health Sci.*, 3 (2015) 1–9.
- [10] S. Sobhanardakani, H. Parvizmosaed, E. Olyaie, Heavy metals removal from waste waters using organic solid waste-rice husk, *Environ. Sci. Pollut. Res.*, 20 (2013) 5265–5271.
- [11] S. Chakraborty, S. Chowdhury, P. Das, Adsorption of crystal violet from aqueous solution onto NaOH-modified rice husk, *Carb. Polym.*, 84 (2011) 1533–1541.
- [12] D. Ghosh, M.K. Sinha, M.K. Purkait, A comparative analysis of low-cost ceramic membrane preparation for effective fluoride removal using hybrid technique, *Desalination*, 327 (2013) 2–13.
- [13] R. Malaisamy, A. Talla-Nwafo, K.L. Jones, Poly electrolyte modification of nano filtration membrane for selective removal of monovalent anions, *Sep. Purif. Technol.*, 77 (2011) 367–374.
- [14] M. Tahaikt, I. Achary, M.A. Menkouchi Sahli, Z. Amor, M. Taky, A. Alami, A. Boughriba, M. Hafsi, A. Elmidaoui, De-fluorination of Moroccan groundwater by electro dialysis: Continuous operation, *Desalination*, 18 (2006) 215–220.
- [15] Y. Guo, K. Yu, Z. Wang, H. Xu, Effects of activation conditions on preparation of porous carbon from rice husk, *Carbon*, 41 (2000) 1645–1687.
- [16] Z. Hu, M.P. Srinivasan, Preparation of high-surface-area activated carbon from coconut shell, *Micro porous Meso porous Mater.*, 27 (1999) 11–18.
- [17] Y. Liu, Y. Guo, Y. Zhu, D. An, W. Gao, Z. Wang, Y. Ma, Z. Wang, A sustainable route for the preparation of activated carbon and silica from rice husk ash, *J. Hazard. Mater.*, 186 (2011) 1314–1319.
- [18] S. Chakraborty, M. Roy, P. Pal, Removal of fluoride from contaminated groundwater by cross flow nano filtration: Transport modeling and economic evaluation, *Desalination*, 313 (2013) 115–124.
- [19] I.A.W. Tan, A.L. Ahmad, B.H. Hameed, Adsorption isotherms, kinetics, thermodynamics and desorption studies of 2, 4, 6-trichlorophenol on oil palm empty fruit bunch-based activated carbon, *J. Hazard. Mater.*, 164 (2009) 473–482.
- [20] S. Chowdhury, P. Das Saha, Artificial neural network (ANN) modeling of adsorption of methylene blue by NaOH-modified rice husk in a fixed-bed column system, *Environ. Sci. Pollut. Res.*, 20 (2013) 1050–1058.
- [21] K. Sinha, S. Chowdhury, P. Das Saha, S. Datta, Modeling of microwave-assisted extraction of natural dye from seeds of *Bixaorellana* (Annatto) using response surface methodology (RSM) and artificial neural network (ANN), *Ind. Crops Products*, 41 (2013) 165–171.
- [22] P. Banerjee, S. Roy Barman, U. Roy, D. Sikder, P. Das, A. Mukhopadhyay, Enhanced degradation of ternary dye effluent by developed bacterial consortium with RSM optimization, ANN modeling and toxicity evaluation, *Desal. Water Treat.*, 72 (2017) 249–265.
- [23] S. Roy, P. Das, S. Sengupta, Treat ability study using novel activated carbon prepared from rice husk: column study, optimization using response surface methodology and mathematical modeling, *Process Saf. Environ. Prot.*, 105 (2017) 184–193.
- [24] S. Roy, P. Das, S. Sengupta, S. Manna, Calcium impregnated activated charcoal: Optimization and efficiency for the treatment of fluoride containing solution in batch and fixed bed reactor, *Process Saf. Environ. Prot.*, 109 (2017) 18–29.
- [25] W.P. Olupot, A. Candia, E. Menya, R. Walozi, Characterization of rice husk varieties in Uganda for bio fuels and their techno-economic feasibility in gasification, *Chem. Eng. Res. Des.*, 107 (2016) 63–72.
- [26] F. Ghorbani, A.M. Sanati, M. Maleki, Production of silica nano particles from rice husk as agricultural waste by environmental friendly technique, *Environ. Stud. Persian Gulf*, 2(1) (2015) 56–65.
- [27] P. Gorthy, M. Pudukottah, Production of silicon carbide from rice husks, *J. Amer. Ceram. Soc.*, 82 (1999) 1393–1400.
- [28] M.A. Girsova, G.F. Golovina, I.A. Drozdova, I.G. Polyakova, T.V. Antropova, Infrared studies and spectral properties of photochromic high silica glasses, *Optica Applicata*, 44 (2014) 337–344.
- [29] A. Sdiri, T. Higashi, S. Bouaziz, M. Benzina, Synthesis and characterization of silica gel from siliceous sands of southern Tunisia, *Arab. J. Chem.*, 7 (2014) 486–493.
- [30] M.N. Khan, A. Sarwar, Determination of point of zero charge of natural and treated adsorbents, *Surf. Rev. Lett.*, 14 (2007) 461–469.
- [31] F. Ghorbani, Y. Habibollah, Z. Mehraban, M.S. Çelik, A.A. Ghoreyshi, M. Anbia, Preparation and characterization of highly pure silica from sedge as agricultural waste and its utilization in the synthesis of mesoporous silica MCM-41, *J. Taiwan Inst. Chem. Eng.*, 44 (2013) 821–828.
- [32] A.W. Tan, A.L. Ahmad, B.H. Hameed, Adsorption of basic dye on high-surface-area activated carbon prepared from coconut husk: equilibrium, kinetic and thermodynamic studies, *J. Hazard Mater.*, 154 (2008) 337–346.
- [33] Y.S. Ho, J.F. Porter, G. McKay, Equilibrium isotherm studies for the sorption of divalent metal ions onto peat: copper, nickel and lead single component systems, *Water Air Soil Pollut.*, 141 (2002) 1–33.